

# Gold-Mediated Expulsion of Dinitrogen from Organic Azides

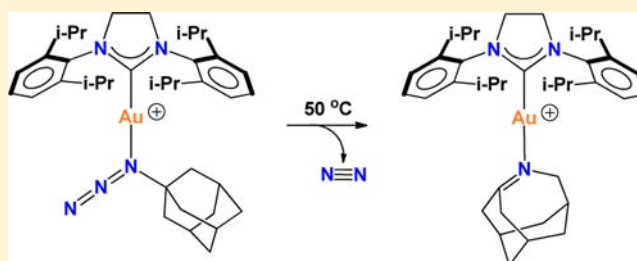
Chandrakanta Dash,<sup>†</sup> Muhammed Yousufuddin,<sup>†</sup> Thomas R. Cundari,<sup>\*,‡</sup> and H. V. Rasika Dias<sup>\*,†</sup>

<sup>†</sup>Department of Chemistry and Biochemistry, The University of Texas at Arlington, Arlington, Texas 76019, United States

<sup>‡</sup>Department of Chemistry, Center for Advanced Scientific Computing and Modeling (CASCaM), University of North Texas, Denton, Texas 76203, United States

**S** Supporting Information

**ABSTRACT:** Organoazides and their nitrogen expulsion chemistry have attracted the attention of many scientists because they serve as a useful source of nitrene fragments and interesting nitrene rearrangement products. Gold-mediated reactions are also of significant current interest. This manuscript describes several important discoveries based at the intersection of these fields. In particular, we report the first isolable gold organoazides [(SIPr)AuN(1-Ad)NN][SbF<sub>6</sub>], [(SIPr)AuN(2-Ad)NN][SbF<sub>6</sub>] and [(SIPr)AuN(Cy)NN][SbF<sub>6</sub>]; SIPr = a *N*-heterocyclic carbene; 1-AdNNN = 1-azidoadamantane; 2-AdNNN = 2-azidoadamantane; CyNNN = azidocyclohexane), and their gold-mediated nitrogen expulsion chemistry, and the isolation of formal nitrene rearrangement products of “1-AdN”, “2-AdN” and “CyN” (including the elusive 4-azahomoadamant-3-ene) as their gold complexes. We have also performed a computational study to understand and explain the observed structure of gold-coordinated 1-AdNNN and 2-AdNNN and their nitrogen elimination pathways, which implies that the conversion of the organoazide complex to the imine is a concerted process without a nitrene/nitrenoid intermediate. Kinetic studies of [(SIPr)AuN(2-Ad)NN][SbF<sub>6</sub>] from 30 to 50 °C indicate that nitrogen elimination is a first-order process. The experimentally determined activation parameters are in good agreement with the calculated values.



## INTRODUCTION

Organoazides (R-NNN; R = alkyl, aryl) have a rich history spanning over a century.<sup>1–6</sup> They are convenient nitrene (R–N) sources. Thermal, photochemical and metal-facilitated routes to nitrenes via the extrusion of dinitrogen from organoazides are known.<sup>4,5,7–10</sup> The nature, use or fate of the resulting nitrenes has been the focus of many investigations. For example, photolysis of 1-AdNNN (1-azidoadamantane; Figure 1, 1) leads to loss of N<sub>2</sub> and formation of a transient intermediate, 4-azahomoadamant-3-ene (3), which was observed spectroscopically with matrix isolation techniques.<sup>11,12</sup>

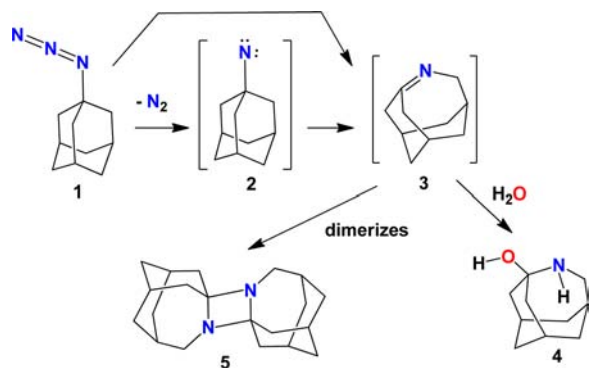


**Figure 1.** Dinitrogen expulsion chemistry of 1-azidoadamantane, 1-AdNNN (1).

Concerted routes and a two-step process involving the nitrene intermediate **2** have both been proposed for the conversion of 1-AdNNN to **3**.<sup>2,4,5,13</sup> Under ambient conditions, the reactive bridgehead imine **3** can be trapped by (a) addition of various reagents to the imine group (e.g., reaction with water leads to 3-hydroxy-4-azahomoadamantane (**4**) or (b) dimerization in a head-to-tail fashion producing **5** (Figure 1).<sup>11,12,14,15</sup> The rearrangement products generated by formal insertion of a nitrene moiety of organoazides have been used in total synthesis and in the synthesis of biologically active molecules such as nicotine.<sup>4</sup>

Photochemical decomposition of 2-AdNNN (2-azidoadamantane; **6**) affords two isomeric products (Figure 2), of which one is a ring-expanded product, 4-azahomoadamant-4-ene (**7**), with an endocyclic imine functionality as in the case of the decomposition of 1-AdNNN, and a second product, 2-iminoadamantane (**8**) with an exocyclic imine group, results from involvement of the  $\alpha$ -H to the azido moiety in the rearrangement process.<sup>14,15</sup>

Lewis acids also mediate dinitrogen expulsion from 1-AdNNN, leading to skeletal rearrangement product **3**, which subsequently reacts with surrounding substrates. For example, AlCl<sub>3</sub> facilitates reactions of 1-AdNNN with aromatic substrates producing arene addition products, 3-aryl-4-azahomoadamantane.<sup>16</sup> Similar chemistry involving other organic azides such as

Received: June 16, 2013

Published: September 20, 2013

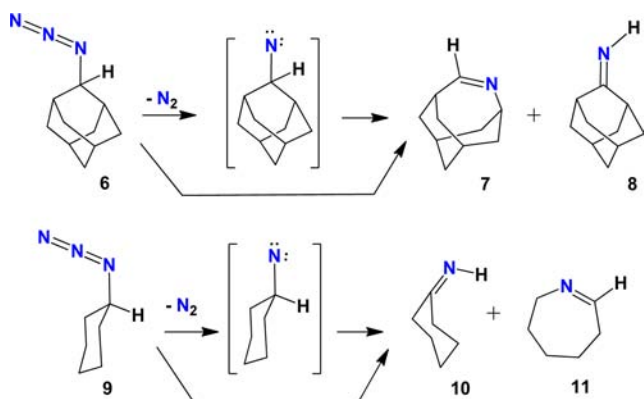


**Figure 2.** Dinitrogen extrusion chemistry 2-azidoadamantane, 2-AdNNN (6) and azidocyclohexane, CyNNN (9).

CyNNN (9, Cy = cyclohexyl) is also known.<sup>16</sup> In the case of CyNNN, nitrogen extrusion followed by rearrangement produces cyclohexanimine (10) in addition to the ring-expanded product, 1-azacyclohept-1-ene (11) (Figure 2).

In this paper, we describe the novel Au(I)-mediated dinitrogen extrusion chemistry of 1-AdNNN, 2-AdNNN and CyNNN and trapping of key rearrangement products, including for the first time 4-azahomoadamant-3-ene (3), as their gold(I) complexes. In addition, isolation of the first gold(I)-organoazide adducts, [(SIPr)AuN(1-Ad)NN][SbF<sub>6</sub>] ([12][SbF<sub>6</sub>]), [(SIPr)AuN(2-Ad)NN][SbF<sub>6</sub>] ([13][SbF<sub>6</sub>]) and [(SIPr)AuN(Cy)NN][SbF<sub>6</sub>] ([14][SbF<sub>6</sub>]) (Figure 3; SIPr = 1,3-bis(2,6-diisopropylphenyl)imidazolin-2-ylidene) is also reported. Density functional theory is used to better understand the chemistry of [12]<sup>+</sup>, [13]<sup>+</sup> and [14]<sup>+</sup>.

Isolable metal-organoazide complexes such as [12][SbF<sub>6</sub>], [13][SbF<sub>6</sub>] and [14][SbF<sub>6</sub>] are of significant interest because many metal-mediated organic syntheses utilizing organoazides likely involve metal-organoazide intermediates. They are, however, rare and the isolation of such species is a challenge due to facile loss of dinitrogen.<sup>5,9,17–29</sup> Among group 11 metals

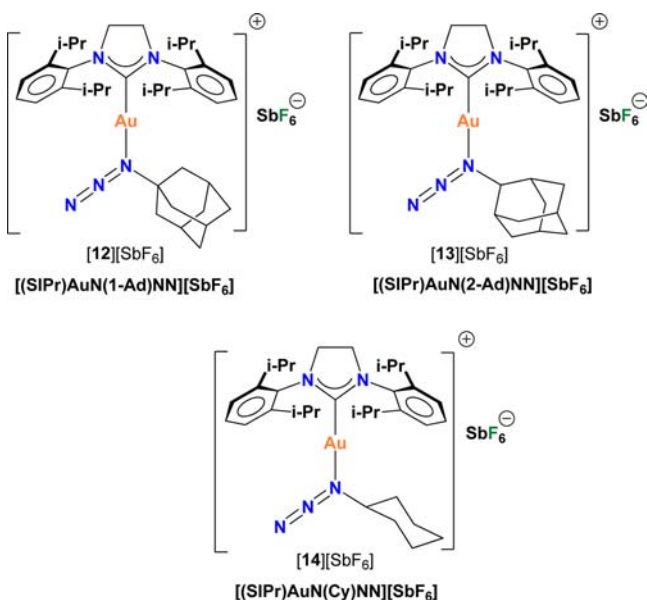


**Figure 3.** Gold(I) complexes of 1-azidoadamantane, 2-azidoadamantane and azidocyclohexane.

(Cu, Ag, Au), there are very few structurally characterized copper- and silver-organoazide complexes<sup>17–19</sup> in the literature; organoazide complexes of gold were unknown prior to this research.

## RESULTS AND DISCUSSION

The gold(I)-organoazide complex [(SIPr)AuN(1-Ad)NN][SbF<sub>6</sub>] ([12][SbF<sub>6</sub>]) can be synthesized from (SIPr)AuCl, AgSbF<sub>6</sub> and 1-AdNNN in CH<sub>2</sub>Cl<sub>2</sub>. [(SIPr)AuN(1-Ad)NN][SbF<sub>6</sub>] is a colorless solid that was characterized by NMR and IR spectroscopy, and X-ray crystallography. The low-temperature (at -20 °C) <sup>13</sup>C{<sup>1</sup>H} NMR spectrum of [12][SbF<sub>6</sub>] in CD<sub>2</sub>Cl<sub>2</sub> exhibited a resonance at δ 188.0 ppm that could be assigned to the Au-C<sub>carbene</sub> carbon, which shows an upfield shift relative to the neutral gold(I)-azide adducts such as (SIPr)AuN<sub>3</sub> (δ 194.66 ppm).<sup>30</sup> The IR spectrum of crystalline [12][SbF<sub>6</sub>] displayed a strong absorption band at 2134 cm<sup>-1</sup>, which corresponds to the asymmetric stretch (*v*<sub>asym</sub>) of the azido group (this band of free 1-azidoadamantane appears at 2088 cm<sup>-1</sup>). There are no reports of gold(I)-organoazide complexes in the literature for a comparison. The tris-(pyrazolyl)borate ligand supported silver(I) adduct, [HB(3,5-(CF<sub>3</sub>)<sub>2</sub>Pz)<sub>3</sub>AgN(1-Ad)NN], however, is known, and it shows the corresponding *v*<sub>asym</sub> stretch at 2120 cm<sup>-1</sup>.<sup>18</sup> DFT calculations also predict an increase in *v*<sub>asym</sub> of the azido group in 1-AdNNN (Calcd 2142 cm<sup>-1</sup>) upon coordination to [(SIPr)Au]<sup>+</sup> (Calcd 2172 cm<sup>-1</sup> for [(SIPr)AuN(1-Ad)NN]<sup>+</sup>).

We isolated two other gold(I)-organoazide complexes [(SIPr)AuN(2-Ad)NN][SbF<sub>6</sub>] ([13][SbF<sub>6</sub>]) and [(SIPr)AuN(Cy)NN][SbF<sub>6</sub>] ([14][SbF<sub>6</sub>]) using a similar synthetic strategy. The <sup>13</sup>C{<sup>1</sup>H} NMR spectra of [13][SbF<sub>6</sub>] and [14][SbF<sub>6</sub>] show the carbene carbon resonance at δ 188.1 and 188.4 ppm, respectively. These values are very similar to that observed for [12][SbF<sub>6</sub>].

The IR spectrum of the crystals of [13][SbF<sub>6</sub>] features a strong absorption band at 2137 cm<sup>-1</sup>. It is the *v*<sub>asym</sub>(N<sub>3</sub>) band, and represents a 50 cm<sup>-1</sup> increase in *v*<sub>asym</sub> value of 2-AdNNN upon coordination to [(SIPr)Au]<sup>+</sup> (the corresponding IR band of the free 2-AdNNN was observed at 2087 cm<sup>-1</sup>). Crystalline [14][SbF<sub>6</sub>] and free CyNNN display *v*<sub>asym</sub>(N<sub>3</sub>) at 2143 and 2085 cm<sup>-1</sup>, respectively. Overall, experimental data and computational studies indicate that the frequency of the asymmetric stretch of these azido groups increases upon coordination to the Lewis acidic gold(I) center.

The identity of gold-organoazide adducts, [12][SbF<sub>6</sub>], [13][SbF<sub>6</sub>] and [14][SbF<sub>6</sub>], were also supported by a [M-SbF<sub>6</sub>]<sup>+</sup> ion peak in ESI-MS mass spectra. Interestingly, all these adducts also displayed ESI-MS peaks corresponding to the nitrogen extrusion product [M-SbF<sub>6</sub>-N<sub>2</sub>]<sup>+</sup>. Solid samples of [12][SbF<sub>6</sub>], [13][SbF<sub>6</sub>] and [14][SbF<sub>6</sub>] can be handled in air for short periods, but they decompose slowly in solution, especially when exposed to air or light. Compound [12][SbF<sub>6</sub>] is relatively less stable than [13][SbF<sub>6</sub>] and [14][SbF<sub>6</sub>] particularly in chlorinated solvents such as CDCl<sub>3</sub> and CD<sub>2</sub>Cl<sub>2</sub>. We have also observed the appearance of bubbles (presumably N<sub>2</sub> resulting from decomposition of metal-bound organoazide) on crystals of [12][SbF<sub>6</sub>], [13][SbF<sub>6</sub>] and [14][SbF<sub>6</sub>] kept at room temperature protected in hydrocarbon/Paratone-N oil. Note that organoazides like 1-AdNNN in pure form have surprisingly high thermal stability. For example, there are reports of 1-AdNNN showing virtually no decomposition even after 45 h in benzene at 200 °C.<sup>2</sup>

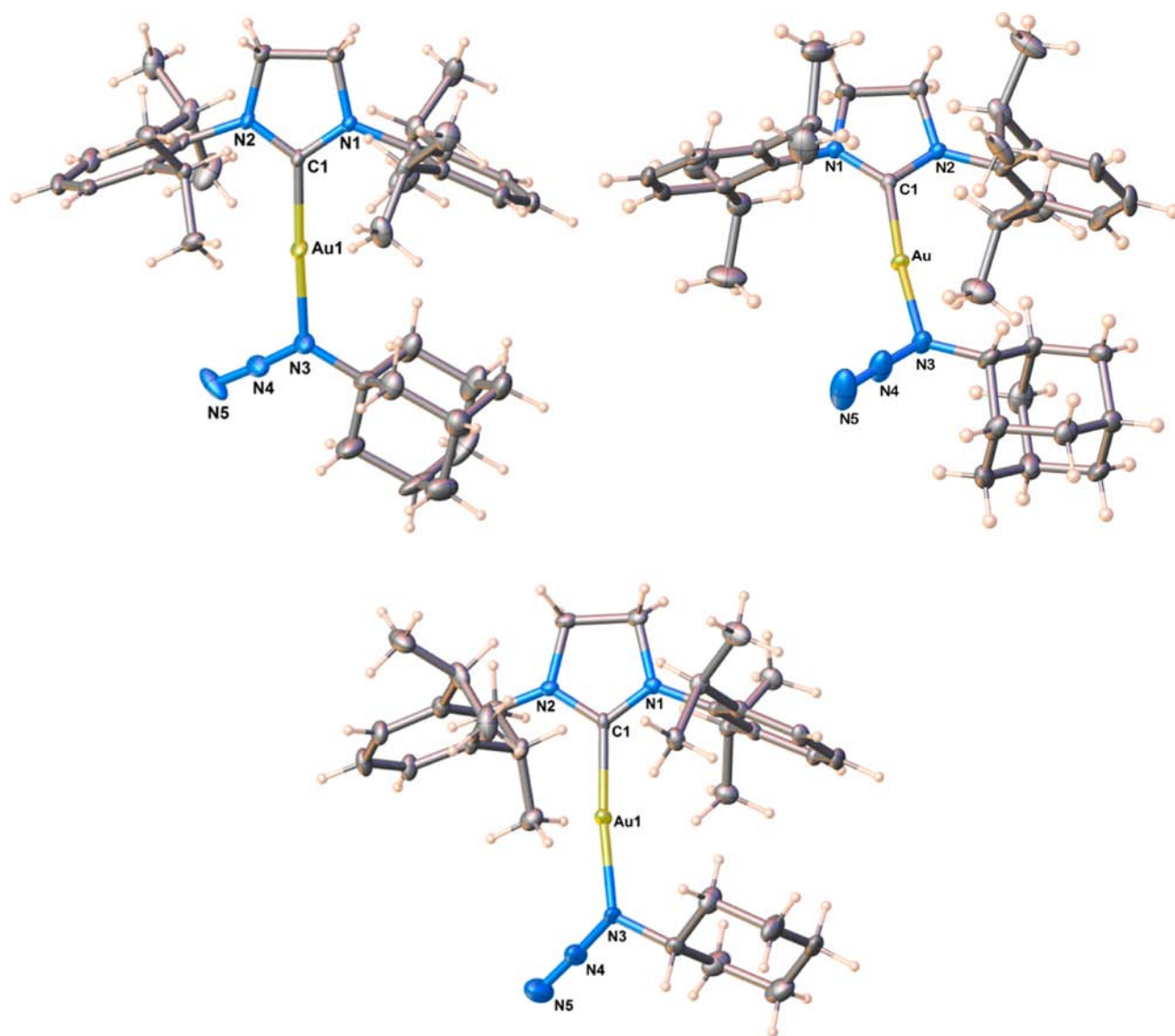


**Figure 4.** Molecular structures of  $[(\text{SIPr})\text{AuN}(1\text{-Ad})\text{NN}]^+$  (top left),  $[(\text{SIPr})\text{AuN}(2\text{-Ad})\text{NN}]^+$  (top right) and  $[(\text{SIPr})\text{AuN}(\text{Cy})\text{NN}]^+$  (bottom center) moieties. The  $[\text{SbF}_6]^-$  counterions have been omitted for clarity. There are two chemically similar but crystallographically distinct molecules of  $[(\text{SIPr})\text{AuN}(1\text{-Ad})\text{NN}][\text{SbF}_6]$  ( $[\mathbf{12}][\text{SbF}_6]$ ) and  $[(\text{SIPr})\text{AuN}(\text{Cy})\text{NN}][\text{SbF}_6]$  ( $[\mathbf{14}][\text{SbF}_6]$ ) in each of their asymmetric units.

X-ray crystal structures of the  $[(\text{SIPr})\text{AuN}(1\text{-Ad})\text{NN}]^+$ ,  $[(\text{SIPr})\text{AuN}(2\text{-Ad})\text{NN}]^+$  and  $[(\text{SIPr})\text{AuN}(\text{Cy})\text{NN}]^+$  moieties of  $[\mathbf{12}][\text{SbF}_6]$ ,  $[\mathbf{13}][\text{SbF}_6]$  and  $[\mathbf{14}][\text{SbF}_6]$  are illustrated in Figure 4. In  $[\mathbf{12}][\text{SbF}_6]$  and  $[\mathbf{14}][\text{SbF}_6]$  adducts, there are two chemically similar but crystallographically different molecules in the asymmetric unit. The Au–C<sub>carbene</sub> bond distance in gold(I)–organoazide complexes (average Au–C<sub>carbene</sub> = 1.987 Å in  $[\mathbf{12}][\text{SbF}_6]$  (cf. DFT-optimized Au–C distance of 1.996 Å), 1.993(6) Å in  $[\mathbf{13}][\text{SbF}_6]$ , and average 1.978 Å in  $[\mathbf{14}][\text{SbF}_6]$ ) is marginally longer than the reported Au–C<sub>carbene</sub> bond length of neutral gold(I)–azide complex,  $(\text{SIPr})\text{AuN}_3$  (Au–C<sub>carbene</sub> = 1.961(3) Å).<sup>30</sup> The gold(I) center in  $[(\text{SIPr})\text{AuN}(\text{R})\text{NN}]^+$  adopts an essentially linear geometry and contains  $\kappa^1$ -bonded NNNR groups (R = 1-Ad, 2-Ad, Cy). For example, the C1–Au–N3 angle of  $[\mathbf{13}][\text{SbF}_6]$  is 174.1(3)°. The NNN moiety of these adducts is also linear with NNN angles ranging from 175(3)–178(3)°. Interestingly, the azide moiety coordinates to gold atom through the internal nitrogen atom (alkylated nitrogen atom, N<sub>A</sub>). The Au–N<sub>A</sub> distances of  $[\mathbf{12}][\text{SbF}_6]$  (average 2.065 Å),  $[\mathbf{13}][\text{SbF}_6]$

(1.961(6) Å), and  $[\mathbf{14}][\text{SbF}_6]$  (average 2.055 Å) may be compared to the corresponding distances of the DFT-optimized structures (2.118, 2.120, and 2.110 Å, respectively).

Simulations were performed to understand the preference for bonding to the internal nitrogen of 1-AdNNN. Optimized  $[\mathbf{12}]^+$  was modified to a linkage isomer in which substrate is  $\kappa^1$ -N coordinated via the terminal nitrogen atom ( $[\mathbf{12}\text{-term}]^+$ ; i.e.  $[(\text{SIPr})\text{AuNNN}(1\text{-Ad})]^+$ ) and then geometry optimized at the level of theory the same as for  $[\mathbf{12}]^+$  (Supporting Information); a minimum for  $[\mathbf{12}\text{-term}]^+$ , 5.1 kcal/mol higher in free energy than  $[\mathbf{12}]^+$ , was obtained. Analysis of the quantum/molecular mechanics energy partition suggests that the stability of  $[\mathbf{12}]^+$  versus  $[\mathbf{12}\text{-term}]^+$  is largely electronic in origin. Furthermore, Mulliken population analysis of 1-AdNNN indicates that N<sub>A</sub> is more basic ( $q(\text{N}_A) = -0.22 e^-$ ) than the middle ( $q(\text{N}) = +0.49 e^-$ ) and terminal ( $q(\text{N}) = +0.02 e^-$ ) nitrogens; thus, Lewis acidic  $[(\text{SIPr})\text{Au}]^+$  preferentially coordinates to N<sub>A</sub> despite any steric benefit that may result from  $\kappa^1$ -N-terminal ligation. The preferences for N<sub>A</sub> bonding are consistent with reported proton and lithium ion affinities for organoazides.<sup>18</sup> Additionally,

previous research by Dias et al. shows  $\kappa^1$ -N-terminal ligation for the smaller copper and  $\kappa^1$ -N-terminal ligation for larger silver congeners in  $[\text{HB}(3,5\text{-}(\text{CF}_3)_2\text{Pz})_3]\text{CuNNN}(1\text{-Ad})$  and  $[\text{HB}(3,5\text{-}(\text{CF}_3)_2\text{Pz})_3]\text{AgN}(1\text{-Ad})\text{NN}$  adducts.<sup>18</sup> The preference for  $\kappa^1$ -N-terminal ligation in  $[\mathbf{12}][\text{SbF}_6]$ ,  $[\mathbf{13}][\text{SbF}_6]$  and  $[\mathbf{14}][\text{SbF}_6]$  is significant in that this linkage isomer is ideally set up for loss of  $\text{N}_2$  and subsequent nitrenoid reactivity.

As noted earlier, organoazides serve as precursors for nitrenoid fragments via photolytic or thermolytic loss of dinitrogen. Certain metal ions are also known to facilitate this process. In fact, the stabilization of resulting nitrene on a metal center and its direct transfer to various external substrates without the skeletal rearrangement are also known.<sup>31–33</sup> For example, nickel-<sup>34,35</sup> and iron<sup>36</sup>-mediated transfer of the nitrene fragment “1-AdN” (**2**) to CO and isocyanides leading to isocyanates and carbodiimides, respectively, is known. Copper-catalyzed insertion of “1-AdN” to inert C–H bonds of hydrocarbons has also been reported.<sup>37,38</sup> These processes involve the use of 1-AdNNN as the nitrene precursor, and the reactions proceed via nickel-, iron-, and copper-stabilized nitrene intermediates.<sup>36,37,39</sup> Several reports on gold-mediated nitrene transfer reactions leading to olefin aziridination and saturated C–H bond activations have also appeared in the literature.<sup>40–42</sup> Although these processes do not involve organoazides as the nitrene precursor, they illustrate the growing importance of gold in nitrene chemistry.

Thus, with three isolable gold(I) organoazide complexes in hand, we set out to explore their nitrogen extrusion chemistry and the resulting products. There were indications, as noted above, that the dinitrogen could be driven out of  $[\mathbf{12}][\text{SbF}_6]$ ,  $[\mathbf{13}][\text{SbF}_6]$  and  $[\mathbf{14}][\text{SbF}_6]$  under relatively mild conditions. For example, mass spectroscopic data suggested the existence of metal-coordinated, nitrogen-extrusion products. Indeed, upon thermolysis at 50 °C, a dichloromethane–hexane solution of  $[\mathbf{12}][\text{SbF}_6]$  loses dinitrogen readily to form a unique gold(I)-bonded rearrangement product  $[(\text{SIPr})\text{Au}(4\text{-azahomoadamant-3-ene})][\text{SbF}_6]$  ( $[\mathbf{15}][\text{SbF}_6]$ ) (Figure 5), concomitant with C–C bond breakage and new C–N bond formation. The 4-azahomoadamant-3-ene (**3**) is a reactive intermediate that results from the elimination of dinitrogen from 1-AdNNN followed by the skeletal rearrangement of the resulting nitrene.<sup>2,11,12</sup> It has been observed spectroscopically, dimerizes easily to **5**, and has been “trapped” by addition of reagents across the double bond. Here, however, we provide for the first time direct observation of 4-azahomoadamant-3-ene on a metal fragment.

$[(\text{SIPr})\text{Au}(4\text{-azahomoadamant-3-ene})][\text{SbF}_6]$  ( $[\mathbf{15}][\text{SbF}_6]$ ) was characterized by NMR and IR spectroscopy, elemental analysis, and X-ray diffraction studies. It is a colorless, crystalline product and can be handled in air for short periods of time but decomposes slowly in dichloromethane when exposed to air. The molecular structure of  $[\mathbf{15}][\text{SbF}_6]$  is depicted in Figure 6. Unfortunately, the 4-azahomoadamant-3-ene moiety in this structure shows positional disorder (Figure S4, Supporting Information), and therefore, it is not suitable for detailed analyses of the bond distances and angles. Nevertheless, existence of the basic skeleton and the coordination via the imine nitrogen atom are clear from the data, and is corroborated by DFT simulations as discussed below (e.g., C–N and C=N distances of gold-bound 4-azahomoadamant-3-ene are av. 1.46(2) and 1.285(13) Å, respectively while the corresponding DFT-optimized distances are 1.493 and 1.311

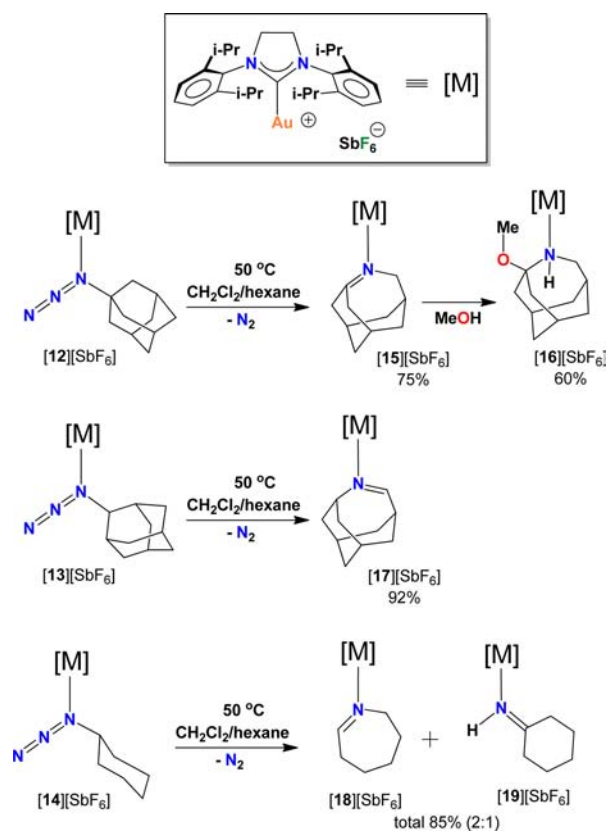


**Figure 5.** Nitrogen extrusion chemistry of gold(I)-bonded organoazide complexes.

Å). These parameters may also be compared to the gold-bound 4-azahomoadamant-4-ene ( $[\mathbf{17}][\text{SbF}_6]$ ) data described later.

We performed a thorough spectroscopic study to confirm the identity of  $[\mathbf{15}][\text{SbF}_6]$ . Its  $^{13}\text{C}$  NMR spectrum in  $\text{CD}_2\text{Cl}_2$  shows two downfield resonances; the one at  $\delta$  204.9 ppm can be assigned as the carbon resonance of  $\text{C}=\text{N}$ , while the second peak at  $\delta$  192.9 ppm is due to the  $\text{C}_{\text{carbene}}-\text{Au}$ . The  $^1\text{H}/^{13}\text{C}$  HMBC spectrum provides further support for this assignment as the  $^{13}\text{C}$  peak at  $\delta$  204.9 ppm shows coupling with protons in 4-azahomoadamant-3-ene moiety, and the resonance at  $\delta$  192.9 ppm for carbene carbon peak displays coupling with the  $\text{CH}_2$  protons at  $\delta$  4.21 ppm in the imidazolin-2-ylidene ring (Supporting Information). Furthermore, a DEPT-135 spectrum yielded seven  $\text{CH}_2$  signals, consistent with the proposed structure. The ESI-MS of  $[\mathbf{15}][\text{SbF}_6]$  in  $\text{CH}_3\text{CN}$  showed a peak at  $m/z$  736.3891 Da, corresponding to the molecular ion peak  $[\mathbf{15}]^+$ . Interestingly, ESI-MS of  $[\mathbf{15}][\text{SbF}_6]$  in MeOH also showed a molecular ion peak at  $m/z$  768.4156 Da, which suggested that the methanol addition product,  $[(\text{SIPr})\text{Au}(\text{NHC}_{10}\text{H}_{15}\text{OMe})]^+$  ( $[\mathbf{16}]^+$ ) may be accessible. Indeed, we were able to synthesize  $[(\text{SIPr})\text{Au}(3\text{-methoxy-4-azahomoadamantane})][\text{SbF}_6]$  ( $[\mathbf{16}][\text{SbF}_6]$ ) independently by treating  $[(\text{SIPr})\text{Au}(4\text{-azahomoadamant-3-ene})][\text{SbF}_6]$  ( $[\mathbf{15}][\text{SbF}_6]$ ) with methanol. Notably, MeOH reacts with the gold-bound imine group, and the resulting product also remains coordinated to the gold. The X-ray crystal structure of  $[\mathbf{16}][\text{SbF}_6]$  is illustrated in Figure 6. It clearly shows presence of the methoxy group on the bridgehead carbon and the formation of the amine and the existence of 4-azahomoadamantane skeleton. The gold atom coordinates to the 3-methoxy-4-azahomoadamantane fragment via the nitrogen

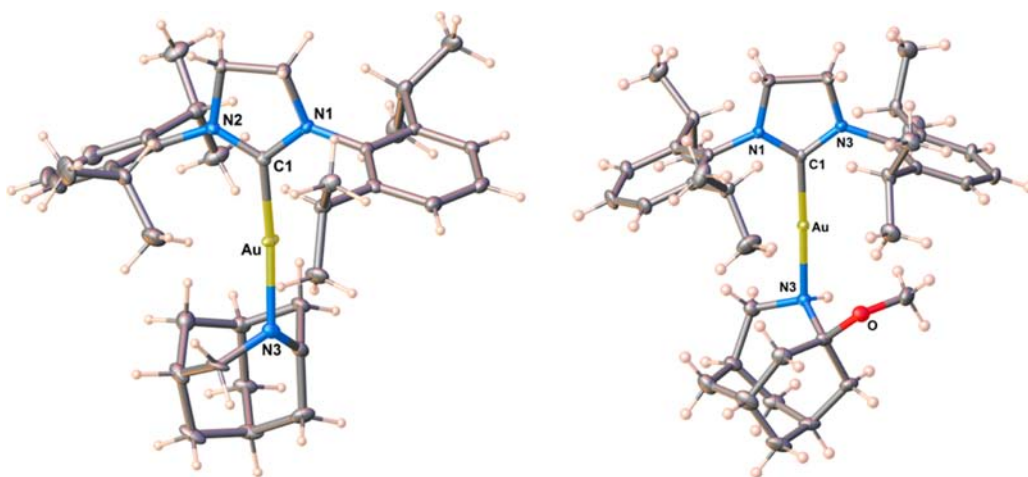


**Figure 6.** Molecular structures of  $[(\text{SIPr})\text{Au}(4\text{-azahomoadamant-3-ene})]^+$  ( $[\mathbf{15}]^+$ , left),  $[(\text{SIPr})\text{Au}(3\text{-methoxy-4-azahomoadamantane})]^+$  ( $[\mathbf{16}]^+$ , right). The  $[\text{SbF}_6]^-$  counterion has been omitted for clarity.

atom rather than the oxygen. The Au–N bond distance (2.112(3) Å is slightly longer than Au–N(imine) distances of  $[\mathbf{15}][\text{SbF}_6]$  (average 2.072 Å) and  $[\mathbf{17}][\text{SbF}_6]$  (described below, 2.064(3) Å).

Density functional theory simulations were performed to better understand the conversion organoazide complexes to their corresponding imines plus  $\text{N}_2$  (Figure 7). Geometry

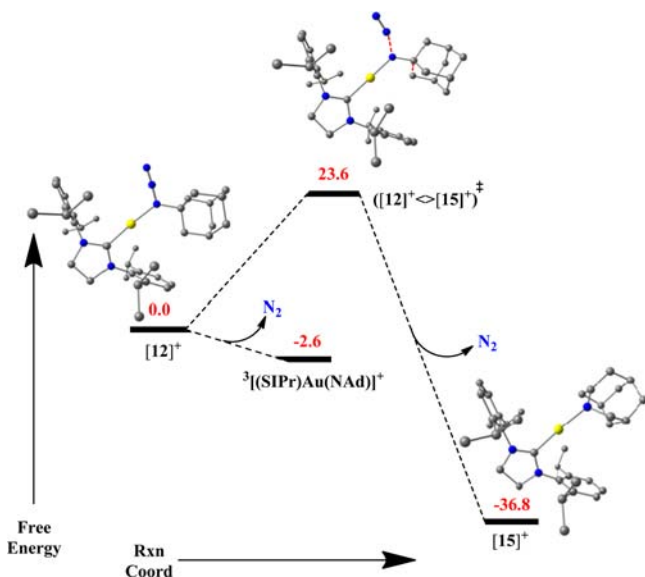


**Figure 7.** DFT computed free energy (red text, in kcal/mol) surface for elimination of  $\text{N}_2$  from  $[\mathbf{12}]^+$  to form  $[\mathbf{15}]^+$ .

optimization of singlet  $[\mathbf{12}]^+$  and  $[\mathbf{15}]^+$  yielded minima (Supporting Information) whose structures were in excellent agreement with experiment, supporting the experimental formulations depicted in Figures 5 and 6. Imine complex  $[\mathbf{15}]^+$  plus  $\text{N}_2$  is calculated to be 36.8 kcal/mol exergonic relative to organoazide complex  $[\mathbf{12}]^+$ , consistent with the facility with which  $\text{N}_2$  extrusion from this complex occurs.

Two pathways are modeled for conversion of  $[\mathbf{12}]^+$  to  $[\mathbf{15}]^+$ : (a) first  $\text{N}_2$  loss, formation of a stable gold–nitrene intermediate, then C–N bond formation via alkyl migration, and (b) concerted  $\text{N}_2$  loss and alkyl migration. DFT analysis of the  $[\mathbf{12}]^+ \rightarrow [\mathbf{15}]^+$  reaction coordinate yields several important

conclusions of relevance to the utilization of these and related materials for catalytic C–N bond formation. First, the  $[\mathbf{12}]^+ \rightarrow [\mathbf{15}]^+$  transformation is facile entirely on the singlet surface, with a computed free energy barrier of 23.6 kcal/mol (Figure 7). This contrasts metal-free organoazides, whereby nitrogen extrusion requires a “spin flip” due to the triplet ground state of the nitrene product<sup>43</sup> and which engenders a significant barrier to  $\text{N}_2$  loss. Besora and Harvey calculate the minimum energy crossing point for  $\text{N}_2$  expulsion from methyl azide at nearly 40 kcal/mol using high-level correlated methods.<sup>43</sup> In a matrix isolation study of the “apo” AdNNN reaction by Michl and co-workers,<sup>12</sup> triplet NAd was deduced to lie off the reaction coordinate. While the large atomic number of gold may facilitate formally spin-forbidden processes, there may be no need to invoke such a mechanism here. However, we cannot categorically rule it out. Geometry optimization of the triplet state of  $[\mathbf{12}]^+$  converges to triplet  $[(\text{SIPr})\text{Au}(\text{NAd})]^+$  with  $\text{N}_2$  in the outer coordination sphere, Figure 7. DFT simulations suggest a triplet ground state for  $[(\text{SIPr})\text{Au}(\text{NAd})]^+$ , which is 2.6 kcal/mol lower in free energy than  $[\mathbf{12}]^+$ , and which has  $\sim 1.6$  unpaired electrons on the nitrene N.

We also investigated the thermolysis of the other two gold(I)-bound organoazide complexes, namely,  $[(\text{SIPr})\text{AuN}(2\text{-Ad})\text{NN}][\text{SbF}_6]$  ( $[\mathbf{13}][\text{SbF}_6]$ ) and  $[(\text{SIPr})\text{AuN}(\text{Cy})\text{NN}][\text{SbF}_6]$  ( $[\mathbf{14}][\text{SbF}_6]$ ). As mentioned earlier, due to the presence of an  $\alpha$ -H atom in the 2-azidoadamantane and azidocyclohexane, there is a possibility of forming two types of isomeric products. Brinker et al. showed that the photolysis of 2-azidoadamantane entrapped in  $\alpha$ - and  $\beta$ -cyclodextrin affords the ring-expanded (endocyclic) imine **7** (4-azahomoadamant-4-ene) as the major product and an exocyclic imine 2-iminoadamantane in minor quantities (**8**).<sup>14</sup> The thermolysis of gold(I)-bound 2-azidoadamantane (i.e.,  $[\mathbf{13}][\text{SbF}_6]$ ) gave only the ring-expanded imine product  $[(\text{SIPr})\text{Au}(4\text{-azahomoadamant-4-ene})][\text{SbF}_6]$  ( $[\mathbf{17}][\text{SbF}_6]$ ) in near quantitative yield (92%) (Figure 5). Computations for  $[\mathbf{13}]^+$  isolated two  $\text{N}_2$  expulsion transition states (geometries in Supporting Information), one leading to endocyclic imine  $[\mathbf{17}]^+$  and another to the isomeric exocyclic imine complex. The latter barrier was computed to be higher in free energy by  $\sim 1$  kcal/mol ( $\Delta G_{\text{endo}}^{\ddagger} = 26.3$  versus  $\Delta G_{\text{exo}}^{\ddagger} = 27.1$  kcal/mol), consistent with the experimental selectivity. In contrast to  $[\mathbf{15}][\text{SbF}_6]$  (which results from the thermolysis of gold(I)-bound 1-azidoadamant-

tane), complex  $[17][\text{SbF}_6]$  is an air- and moisture-stable solid, probably because  $[17][\text{SbF}_6]$  (unlike  $[15][\text{SbF}_6]$ ) does not contain a reactive bridgehead imine.

The carbene carbon resonance in  $^{13}\text{C}$  NMR spectrum of  $[17][\text{SbF}_6]$  in  $\text{CDCl}_3$  appears at  $\delta$  190.6 ppm. The imine  $\text{C}=\text{N}$  carbon resonance was observed at  $\delta$  186.3 ppm. The ESI-MS of  $[17][\text{SbF}_6]$  in MeOH showed a peak at  $m/z$  736.3884 Da, corresponding to the molecular ion peak. However, unlike the ESI-MS of  $[15][\text{SbF}_6]$ , we did not observe any methanol addition product to the imine bond of  $[17][\text{SbF}_6]$  in the mass spectrum.

Molecular structure of  $[17][\text{SbF}_6]$  is illustrated in Figure 8. It shows that gold coordinates to the 4-azahomoadamantane-4-

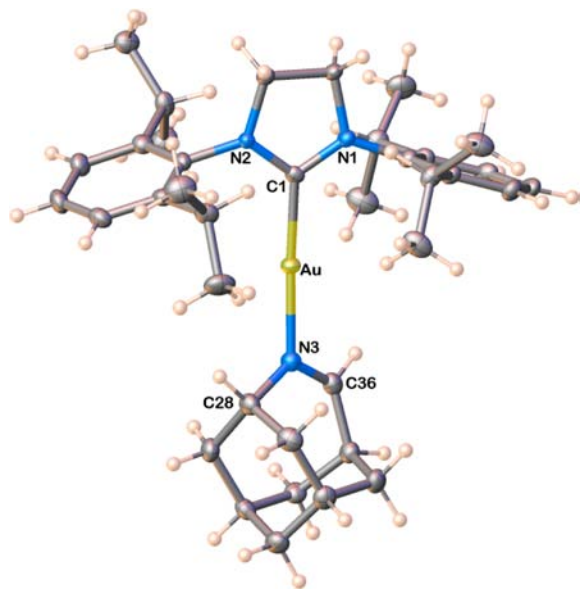


**Figure 8.** Molecular structure of  $[(\text{SIPr})\text{Au}(4\text{-azahomoadamantane-4-ene})]^+$ . The  $[\text{SbF}_6]^-$  counterion has been omitted for clarity.

ene via the imine nitrogen atom. The gold atom is linear with  $\text{C1-Au-N3}$  angle of  $176.20(11)^\circ$ . The  $\text{C}=\text{N}$  bond distance

( $\text{N3-C36}$ ) of  $1.281(4)$  Å in  $[17][\text{SbF}_6]$  is significantly shorter than the  $\text{N3-C28}$  ( $\text{C-N}$  single) bond distance ( $1.496(4)$  Å), as expected. The gold(I)-coordinated nitrogen atom is planar (sum of the angles at  $\text{N3} = 359^\circ$ ). The related  $\text{C-N}$ ,  $\text{C}=\text{N}$  distances of the DFT-optimized structure are 1.293 and 1.505 Å, respectively. The experimental and DFT computed  $\text{Au-N}$  distances are also in good agreement:  $2.064(3)$  and  $2.090$  Å, respectively.

The dinitrogen extrusion chemistry of gold(I)-bonded azidocyclohexane  $[14][\text{SbF}_6]$  adduct was also investigated. It afforded an isomeric mixture of two nitrene rearrangement products, *i.e.*, a ring-expanded seven-membered imine— $[(\text{SIPr})\text{Au}(1\text{-azacyclohept-1-ene})][\text{SbF}_6]$  ( $[18][\text{SbF}_6]$ )—and a six-membered imine product— $[(\text{SIPr})\text{Au}(\text{cyclohexanimine})][\text{SbF}_6]$  ( $[19][\text{SbF}_6]$ ) (Figure 5). It has been reported by Kreher and Jäger that azidocyclohexane in the presence of  $\text{AlCl}_3$  and benzene at  $50^\circ\text{C}$  forms two rearrangement products, the ring-expanded product **11** and cyclohexanimine **10** (Figure 2), in addition to cyclohexylbenzene.<sup>44</sup>  $^1\text{H}$  NMR spectra indicate the presence of two isomers  $[18][\text{SbF}_6]$  and  $[19][\text{SbF}_6]$  at about 2:1 molar ratio. The presence of 1-azacyclohept-1-ene in  $[18][\text{SbF}_6]$  was supported from DEPT-135  $^{13}\text{C}$  NMR data (a resonance at 184.5 ppm), whereas the cyclohexanimine fragment in  $[19][\text{SbF}_6]$  gave rise to a NH peak at  $3296\text{ cm}^{-1}$  in the IR. High-resolution ESI-MS gave a strong peak at  $m/z$  684.3609 Da, indicating the presence of a  $[(\text{SIPr})\text{Au}(\text{NC}_6\text{H}_{11})]^+$  species. Further confirmation was obtained from X-ray crystallography (Figure 9). Interestingly, and also unfortunately, both isomers  $[18][\text{SbF}_6]$  and  $[19][\text{SbF}_6]$  cocrystallize, and the 1-azacyclohept-1-ene and cyclohexanimine moieties occupy the same ligand site in about 33% and 67% occupancy, respectively (Figure S6, Supporting Information). With appropriate restraints, it is possible to resolve the two species, but the resulting structure is less than ideal for detailed analysis of metric parameters. The basic structural features, however, are clear with both adducts featuring essentially linear, two-coordinate gold atoms bonded to the carbene carbon and to the nitrogen atom of either the seven-membered heterocycle ( $[18][\text{SbF}_6]$ ) or cyclohexanimine ( $[19][\text{SbF}_6]$ ). The IR spectrum of this mixture shows a band at

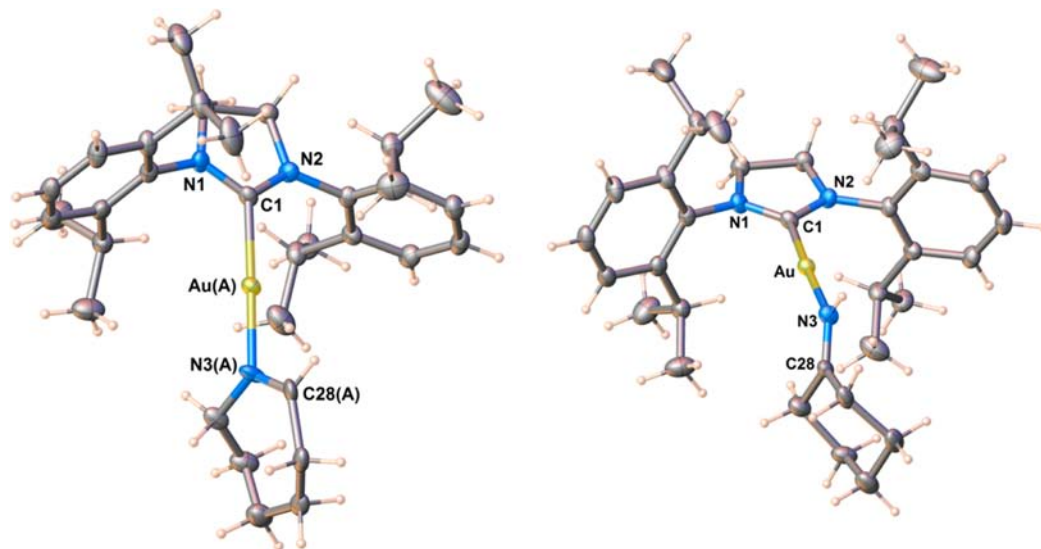


**Figure 9.** Molecular structures of  $[(\text{SIPr})\text{Au}(1\text{-azacyclohept-1-ene})]^+$  (left) and  $[(\text{SIPr})\text{Au}(\text{cyclohexanimine})]^+$  (right). The  $[\text{SbF}_6]^-$  counterion has been omitted for clarity.

3296  $\text{cm}^{-1}$ , which is perhaps due to the NH group. For comparison,  $\text{Os}_3(\text{CO})_{11}$ (cyclohexanimine) (NH peak at 3323  $\text{cm}^{-1}$ ), which contains the cyclohexanimine moiety on osmium, is known.<sup>45</sup>

We have also carried out kinetic studies for the conversion of the complex  $[\mathbf{13}][\text{SbF}_6]$  to gold(I)-bonded rearrangement product  $[\mathbf{17}][\text{SbF}_6]$ . Compound  $[\mathbf{13}][\text{SbF}_6]$  rather than the other adducts (such as  $[\mathbf{12}][\text{SbF}_6]$ ) was chosen for this experiment because it produces  $[\mathbf{17}][\text{SbF}_6]$  cleanly in relatively higher yield, gives a much simpler  $^1\text{H}$  NMR spectrum for the crude reactant–product mixture, and has well-separated reactant and product resonances for  $[\mathbf{13}][\text{SbF}_6]$  and  $[\mathbf{17}][\text{SbF}_6]$  that can be monitored easily. The thermolysis of  $[\mathbf{13}][\text{SbF}_6]$  in  $\text{CDCl}_3$  at 30–50 °C was monitored by following the disappearance of a proton signal of  $[\mathbf{13}][\text{SbF}_6]$  at  $\delta$  3.89 ppm. The data obtained at 50 °C plotted on a logarithmic scale show a first-order decay ( $k_{\text{obs}} = 2.4(1) \times 10^{-4} \text{ s}^{-1}$ , Figure S8, Supporting Information). An Eyring plot of the first-ordered rate constants was determined for the thermolysis of  $[\mathbf{13}][\text{SbF}_6]$  over a temperature range of 30 to 50 °C gave activation parameters,  $\Delta H^\ddagger = 21.5(2) \text{ kcal/mol}$  and  $\Delta S^\ddagger = -8.6(7) \text{ eu}$  (1 eu = 1 cal/(mol K)). Kinetic studies of metal organic azides have been reported for comparisons, although none of these involve gold complexes.<sup>9,20,22,26</sup>

In summary, we have demonstrated for the first time that it is possible to stabilize organoazide complexes of gold(I). We have also found that the  $\text{N}_2$  expulsion from gold-bound 1-AdNNN, 2-AdNNN and CyNNN leads to rearrangement products featuring endocyclic imine moieties in a seven-membered heterocyclic framework as in 4-azahomoadamant-3-ene, 4-azahomoadamant-4-ene, and 1-azacyclohept-1-ene or exocyclic groups as in cyclohexanimine. All these products of dinitrogen extrusion have been isolated as their N-coordinated  $[(\text{SIPr})\text{Au}]^+$  adducts. Furthermore, addition of methanol across the gold-bound imine functionality of 4-azahomoadamant-3-ene was also demonstrated, and the structure was established using X-ray crystallography. Currently, we are exploring the nitrene transfer chemistry of these rare gold(I)–organoazides and the related coinage metal-catalyzed processes.

## EXPERIMENTAL SECTIONS

**General Procedures.** All manipulations were carried out under an atmosphere of dry nitrogen, using standard Schlenk techniques or in a glovebox. Solvents were purchased from commercial sources, purified using an Innovative Technology SPS-400 PureSolv solvent drying system or using established solvent drying procedures, and degassed by the freeze–pump–thaw method twice prior to use. Glassware was oven-dried at 150 °C overnight. One-dimensional (1D) and 2D NMR spectral data were recorded at 253 or 298 K on a JEOL Eclipse 500 spectrometer. Proton and carbon chemical shifts are reported in ppm and are referenced using the residual proton and carbon signals of the deuterated solvent. NMR annotations used: br = broad, d = doublet, m = multiplet, s = singlet, t = triplet, sept = septet. Infrared spectra were recorded on a Bruker FT-IR containing ATR attachment operating at 2  $\text{cm}^{-1}$  spectral resolution. IR spectroscopic data were collected as a neat sample (crystals). The relative intensities of the peaks are denoted by: s = strong, m = medium, and w = weak. Herein, we use abbreviations based on IUPAC guidelines, that is,  $\nu$  for frequency and  $\bar{\nu}$  for wavenumber. For HR-ESI-MS analysis, a stock solution was prepared by using 10% of dichloromethane in MeOH or  $\text{CH}_3\text{CN}$ . Elemental analyses were performed by Intertek Pharmaceutical Services, U.S.A. Melting points were obtained on a Mel-Temp II apparatus using samples sealed in capillaries under nitrogen. The  $(\text{SIPr})\text{AuCl}$ ,<sup>46</sup> 2-azidoadamantane,<sup>47</sup> and azidocyclohexane<sup>48</sup> were synthesized using literature procedures. 1-Azidoadamantane and

AgSbF<sub>6</sub> were purchased from Sigma-Aldrich and used without further purification. Note that organic azides are potentially explosive substances. Samples should be handled with care.

**$[(\text{SIPr})\text{AuN}(1\text{-Ad})\text{NN}][\text{SbF}_6]$  ( $[\mathbf{12}][\text{SbF}_6]$ ).** Solid  $(\text{SIPr})\text{AuCl}$  (0.061 g, 0.098 mmol), AgSbF<sub>6</sub> (0.034 g, 0.098 mmol) and 1-azidoadamantane (0.017 g, 0.098 mmol) were placed in a 50-mL Schlenk flask. To this mixture, dichloromethane (~8 mL) was added at –18 °C (using ice/acetone bath), and the solution was stirred for 1 h. The resulting mixture was filtered through a pad of Celite *via* cannula, and the filtrate was concentrated to ~3 mL under reduced pressure. The concentrated solution was layered with hexane (~8 mL) and kept in a refrigerator at –10 °C to obtain colorless, prism-shaped crystals of  $[(\text{SIPr})\text{AuN}(1\text{-Ad})\text{NN}][\text{SbF}_6]$  (0.073 g, 74% yield).  $^1\text{H}$  NMR ( $\text{CD}_2\text{Cl}_2$ , 500.16 MHz, 253 K):  $\delta$  7.45 (t, 2H,  $^3J_{\text{HH}} = 8 \text{ Hz}$ ,  $\text{C}_6\text{H}_3$ ), 7.28 (d, 4H,  $^3J_{\text{HH}} = 8 \text{ Hz}$ ,  $\text{C}_6\text{H}_3$ ), 4.23 (s, 4H,  $\text{CH}_2$ ), 3.00 (sept, 4H,  $^3J_{\text{HH}} = 6.9 \text{ Hz}$ ,  $\text{CH}(\text{CH}_3)_2$ ), 2.02 (s, 3H, Ad), 1.57 (m, 3H, Ad), 1.37 (m, 4H, Ad), 1.35 (m, 29H,  $\text{CH}(\text{CH}_3)_2 + \text{Ad}$ ).  $^{13}\text{C}\{^1\text{H}\}$  NMR ( $\text{CD}_2\text{Cl}_2$ , 125.77 MHz, 253 K):  $\delta$  188.0 (Au–N $\overline{\text{C}}\text{N}$ ), 146.8, 133.2, 130.6, 124.9, 67.7, 54.0, 41.6, 34.7, 30.1, 29.0, 25.3, 24.0. IR (crystals, ATR)  $\text{cm}^{-1}$ : 2954 s, 2922 s, 2854 s, 2134 s (N<sub>3</sub>), 1589 w, 1518 s, 1463 s, 1384 w, 1364 w, 1348 w, 1328 w, 1285 s, 1267 m, 1229 w, 1202 m, 1180 m, 1104 w, 1057 m, 1044 m, 1016 w, 966 w, 936 w, 898 w, 806 m, 760 m, 737 s, 706 w, 681 w, 654 s, 624 w, 578 w, 548 w. A satisfactory elemental analysis could not be obtained despite several attempts. However, the elemental analysis data are consistent with the species formed after loss of N<sub>2</sub>: Anal. Calcd for  $\text{C}_{37}\text{H}_{53}\text{N}_3\text{F}_6\text{AuSb}$ : C, 44.39; H, 5.34; N, 7.00 and for N<sub>2</sub> extrusion product  $\text{C}_{37}\text{H}_{53}\text{N}_3\text{F}_6\text{AuSb}$ : C, 45.69; H, 5.49; N, 4.32. Found: C, 45.63; H, 5.11; N, 4.12%. HR-ESI-MS (positive ion, MeOH)  $m/z$ : 764.3959  $[\text{M} - \text{SbF}_6]^+$  (calcd 764.3966); 736.3899  $[\text{M} - \text{SbF}_6 - \text{N}_2]^+$  (calcd 736.3905).  $[(\text{SIPr})\text{AuN}(1\text{-Ad})\text{NN}][\text{SbF}_6]$  is a colorless, air- and moisture-sensitive solid. The solid samples showed  $\bar{\nu}_{\text{asym}}(\text{N}_3)$  band for azido species in the IR spectrum even after storing in a sealed container for several days under inert atmosphere at –30 °C refrigerator, but in  $\text{CH}_2\text{Cl}_2$  and  $\text{CHCl}_3$  solutions of  $[(\text{SIPr})\text{AuN}(1\text{-Ad})\text{NN}][\text{SbF}_6]$  lose dinitrogen slowly at room temperature.

**$[(\text{SIPr})\text{AuN}(2\text{-Ad})\text{NN}][\text{SbF}_6]$  ( $[\mathbf{13}][\text{SbF}_6]$ ).** Solid  $(\text{SIPr})\text{AuCl}$  (0.103 g, 0.165 mmol), AgSbF<sub>6</sub> (0.057 g, 0.164 mmol), and 2-azidoadamantane (0.029 g, 0.165 mmol) were placed in a 50-mL Schlenk flask. To this mixture, was added dichloromethane (~10 mL) at –18 °C (using ice/acetone bath), and the solution was stirred for 1 h. The resulting mixture was filtered through a pad of Celite *via* cannula, and the filtrate was concentrated to ~3 mL under reduced pressure. The concentrated solution was layered with hexane (~6 mL) and kept in a refrigerator at –10 °C to obtain colorless, prism-shaped crystals of  $[(\text{SIPr})\text{AuN}(2\text{-Ad})\text{NN}][\text{SbF}_6]$  (0.129 g, 78% yield).  $^1\text{H}$  NMR ( $\text{CD}_2\text{Cl}_2$ , 500.16 MHz, 298 K):  $\delta$  7.48 (t, 2H,  $^3J_{\text{HH}} = 8 \text{ Hz}$ ,  $\text{C}_6\text{H}_3$ ), 7.30 (d, 4H,  $^3J_{\text{HH}} = 8 \text{ Hz}$ ,  $\text{C}_6\text{H}_3$ ), 4.25 (s, 4H,  $\text{CH}_2$ ), 3.84 (m, 1H, Ad), 3.04 (sept, 4H,  $^3J_{\text{HH}} = 6.9 \text{ Hz}$ ,  $\text{CH}(\text{CH}_3)_2$ ), 1.78 (m, 3H, Ad), 1.62 (br s, 3H, Ad), 1.52 (m, 6H, Ad), 1.37 (m, 26H,  $\text{CH}(\text{CH}_3)_2 + \text{Ad}$ ).  $^1\text{H}$  NMR ( $\text{CDCl}_3$ , 500.16 MHz, 298 K):  $\delta$  7.45 (t, 2H,  $^3J_{\text{HH}} = 8 \text{ Hz}$ ,  $\text{C}_6\text{H}_3$ ), 7.26 (d, 4H,  $^3J_{\text{HH}} = 8 \text{ Hz}$ ,  $\text{C}_6\text{H}_3$ ), 4.32 (s, 4H,  $\text{CH}_2$ ), 3.89 (m, 1H, Ad), 3.06 (sept, 4H,  $^3J_{\text{HH}} = 6.9 \text{ Hz}$ ,  $\text{CH}(\text{CH}_3)_2$ ), 1.76 (m, 3H, Ad), 1.56 (m, 9H, Ad), 1.37 (m, 26H,  $\text{CH}(\text{CH}_3)_2 + \text{Ad}$ ).  $^{13}\text{C}\{^1\text{H}\}$  NMR ( $\text{CD}_2\text{Cl}_2$ , 125.77 MHz, 298 K):  $\delta$  188.1 (Au–N $\overline{\text{C}}\text{N}$ ), 147.1, 133.5, 131.0, 125.3, 71.1,  $\text{CH}_2$  peak overlapped with solvent signal, 36.6, 36.5, 31.8, 31.4, 29.3, 26.9, 26.8, 25.3, 24.3; DEPT-135 NMR 131.0 (+ve), 125.3 (+ve), 71.1 (+ve), 54.3 (–ve), 36.6 (–ve), 36.5 (–ve), 31.8 (+ve), 31.4 (–ve), 29.3 (+ve), 26.9 (+ve), 26.8 (+ve), 25.3 (+ve), 24.3 (+ve). IR (crystals, ATR, selected band)  $\text{cm}^{-1}$ : 2137 (N<sub>3</sub>). A satisfactory elemental analysis could not be obtained after several attempts, but results obtained were closer to a mixture of  $\text{C}_{37}\text{H}_{53}\text{N}_3\text{F}_6\text{AuSb}$  and N<sub>2</sub> loss product  $\text{C}_{37}\text{H}_{53}\text{N}_3\text{F}_6\text{AuSb}$ : Anal. Calcd for  $\text{C}_{37}\text{H}_{53}\text{N}_3\text{F}_6\text{AuSb}$ : C, 44.41; H, 5.34; N, 7.00. Found: C, 44.30; H, 5.10; N, 5.45%. HR-ESI-MS (positive ion, MeOH)  $m/z$ : 764.3964  $[\text{M} - \text{SbF}_6]^+$  (calcd 764.3966); 736.3905  $[\text{M} - \text{SbF}_6 - \text{N}_2]^+$  (calcd 736.3905).  $[(\text{SIPr})\text{AuN}(2\text{-Ad})\text{NN}][\text{SbF}_6]$  is a colorless solid and moderately air sensitive. The solid samples showed  $\bar{\nu}_{\text{asym}}(\text{N}_3)$  band for azido species in the IR spectrum even after storing in a sealed container for several weeks under inert atmosphere at –5 °C.

[(SIPr)Au(Cy)NN][SbF<sub>6</sub>] ([14][SbF<sub>6</sub>]). Azidocyclohexane (0.010 g, 0.082 mmol) in dichloromethane (8 mL) was placed in a 50-mL Schlenk flask together with several pieces of 4 Å molecular sieves and degassed by the freeze–pump–thaw method. The degassed solution of azidocyclohexane in dichloromethane was added to a solid mixture of (SIPr)AuCl (0.051 g, 0.082 mmol) and AgSbF<sub>6</sub> (0.028 g, 0.082 mmol) at –18 °C (using ice/acetone bath). The reaction mixture was stirred for 1 h at –18 °C. The resulting mixture was filtered through a pad of Celite *via* cannula and the filtrate was concentrated to ~2 mL under reduced pressure. The concentrated solution was layered with hexane (~5 mL) and kept in a refrigerator at –10 °C to obtain colorless, platelike crystals of [(SIPr)AuN(Cy)NN][SbF<sub>6</sub>] (0.063 g, 81% yield). <sup>1</sup>H NMR (CD<sub>2</sub>Cl<sub>2</sub>, 500.16 MHz, 298 K): δ 7.48 (t, 2H, <sup>3</sup>J<sub>HH</sub> = 8 Hz, C<sub>6</sub>H<sub>3</sub>), 7.31 (d, 4H, <sup>3</sup>J<sub>HH</sub> = 8 Hz, C<sub>6</sub>H<sub>3</sub>), 4.25 (s, 4H, CH<sub>2</sub>), 3.57 (m, 1H, Cy), 3.04 (sept, 4H, <sup>3</sup>J<sub>HH</sub> = 6.9 Hz, CH(CH<sub>3</sub>)<sub>2</sub>), 1.57 (m, 5H, Cy), 1.35 (d, 24H, <sup>3</sup>J<sub>HH</sub> = 6.9 Hz, CH(CH<sub>3</sub>)<sub>2</sub>), 1.13 (m, 2H, Cy), 0.88 (m, 1H, Cy), 0.70 (m, 2H, Cy). <sup>13</sup>C{<sup>1</sup>H} NMR (CD<sub>2</sub>Cl<sub>2</sub>, 125.77 MHz, 298 K): δ 188.4 (Au–N<sub>3</sub>), 147.2, 133.5, 131.0, 125.2, 67.5, 54.3, 32.9, 29.4, 25.4, 24.5, 24.4, 24.3; DEPT-135 NMR 131.0 (+ve), 125.2 (+ve), 67.5 (+ve), 54.3 (–ve), 32.9 (–ve), 29.4 (+ve), 25.4 (+ve), 24.5 (–ve), 24.4 (–ve), 24.3 (+ve). IR (crystals, ATR) cm<sup>–1</sup>: 2955 s, 2923 s, 2853 s, 2143 s (N<sub>3</sub>), 1590 w, 1512 s, 1463 s, 1385 w, 1366 w, 1348 w, 1327 w, 1282 s, 1187 m, 1143 w, 1103 m, 1058 w, 1018 w, 936 w, 891 m, 813 s, 765 m, 653 s, 623 w, 574 w, 549 m. A satisfactory elemental analysis could not be obtained after having several attempts, but results obtained were closer to a mixture of C<sub>33</sub>H<sub>49</sub>N<sub>3</sub>F<sub>6</sub>AuSb and N<sub>2</sub> loss product C<sub>33</sub>H<sub>49</sub>N<sub>3</sub>F<sub>6</sub>AuSb: Anal. Calcd for C<sub>33</sub>H<sub>49</sub>N<sub>3</sub>F<sub>6</sub>AuSb: C, 41.79; H, 5.21; N, 7.38. Found: C, 41.71; H, 4.95; N, 5.39%. [(SIPr)AuN(Cy)NN][SbF<sub>6</sub>] is a colorless solid. HR-ESI-MS (MeOH) *m/z*: 712.3621 [M – SbF<sub>6</sub>]<sup>+</sup> (calcd 712.3653); 684.3584 [M – N<sub>2</sub> – SbF<sub>6</sub>]<sup>+</sup> (calcd 684.3592). The crystalline solid compounds can be handled in air for short periods. The solid samples showed  $\bar{\nu}_{\text{asym}}$  (N<sub>3</sub>) band for azido species in the IR spectrum even after being kept in a sealed container for several weeks under an inert atmosphere in a –30 °C refrigerator, but the CH<sub>2</sub>Cl<sub>2</sub> and CHCl<sub>3</sub> solutions of [(SIPr)AuN(Cy)NN][SbF<sub>6</sub>] lose dinitrogen slowly at room temperature.

[(SIPr)Au(4-azahomoadamant-3-ene)][SbF<sub>6</sub>] ([15][SbF<sub>6</sub>]). A solution of [(SIPr)AuN(1-Ad)NN][SbF<sub>6</sub>] (0.064 g, 0.064 mmol) in mixed solvent dichloromethane/hexane (~14 mL, 6:1) was placed in a 50-mL Schlenk flask. The reaction mixture was heated at 50 °C for 6 h. The resulting mixture was concentrated to ~2 mL under reduced pressure. The concentrated solution was layered with hexane (~6 mL) and kept in a refrigerator at –10 °C to obtain colorless, platelike crystals of [(SIPr)Au(4-azahomoadamant-3-ene)][SbF<sub>6</sub>] (0.047 g, 75% yield). Mp: 201–209 °C dec <sup>1</sup>H NMR (CD<sub>2</sub>Cl<sub>2</sub>, 500.16 MHz, 298 K): δ 7.46 (t, 2H, <sup>3</sup>J<sub>HH</sub> = 8 Hz, C<sub>6</sub>H<sub>3</sub>), 7.29 (m, 4H, C<sub>6</sub>H<sub>3</sub>), 4.21 (s, 4H, CH<sub>2</sub>), 4.04 (m, 1H, NC<sub>10</sub>H<sub>15</sub>), 3.37 (m, 1H, NC<sub>10</sub>H<sub>15</sub>), 3.05 (m, 4H, CH(CH<sub>3</sub>)<sub>2</sub>), 2.77 (m, 1H, NC<sub>10</sub>H<sub>15</sub>), 2.71 (m, 1H, NC<sub>10</sub>H<sub>15</sub>), 2.62 (m, 1H, NC<sub>10</sub>H<sub>15</sub>), 2.40 (m, 1H, NC<sub>10</sub>H<sub>15</sub>), 2.20 (br s, 2H, NC<sub>10</sub>H<sub>15</sub>), 1.79 (m, 2H, NC<sub>10</sub>H<sub>15</sub>), 1.65 (m, 1H, NC<sub>10</sub>H<sub>15</sub>), 1.57 (m, 1H, NC<sub>10</sub>H<sub>15</sub>), 1.49 (m, 1H, NC<sub>10</sub>H<sub>15</sub>), 1.35 (m, 26H, CH(CH<sub>3</sub>)<sub>2</sub> + NC<sub>10</sub>H<sub>15</sub>). <sup>13</sup>C{<sup>1</sup>H} NMR (CD<sub>2</sub>Cl<sub>2</sub>, 125.77 MHz, 298 K): δ 204.9 (C=N), 192.9 (Au–N<sub>3</sub>), 147.3, 147.2, 134.1, 130.6, 125.1, 125.0, 58.5, 57.7, 54.1, 41.7, 40.5, 36.4, 35.7, 32.0, 31.1, 29.4, 29.3, 29.1, 25.2, 25.1, 24.4, 24.3; DEPT-135 NMR 130.6 (+ve), 125.1 (+ve), 125.0 (+ve), 58.5 (–ve), 57.7 (–ve), 54.1 (–ve), 41.7 (–ve), 40.5 (–ve), 36.4 (+ve), 35.7 (–ve), 32.0 (–ve), 31.1 (+ve), 29.4 (+ve), 29.3 (+ve), 29.1 (+ve), 25.2 (+ve), 25.1 (+ve), 24.4 (+ve), 24.3 (+ve). IR (crystals, ATR) cm<sup>–1</sup>: 2961 m, 2925 m, 2862 m, 1589 m, 1506 s, 1461 s, 1385 w, 1346 w, 1328 w, 1281 s, 1260 s, 1186 w, 1137 w, 1094 s, 1057 s, 1017 s, 935 m, 898 w, 876 w, 804 s, 759 m, 732 w, 707 w, 654 s, 625 m, 579 w, 547 w, 515 w. Anal. Calcd for C<sub>37</sub>H<sub>53</sub>N<sub>3</sub>F<sub>6</sub>AuSb: C, 45.69; H, 5.49; N, 4.32. Found: C, 45.40; H, 5.20; N, 4.04%. HR-ESI-MS (positive ion, CH<sub>3</sub>CN) *m/z*: 736.3891 [M – SbF<sub>6</sub>]<sup>+</sup> {isotope pattern: 736.3891 (100), 737.3926 (44), 738.3966 (9)} (calcd 736.3905); 628.2954 [M – NC<sub>10</sub>H<sub>15</sub> + CH<sub>3</sub>CN – SbF<sub>6</sub>]<sup>+</sup> (calcd 628.2966). HR-ESI-MS (positive ion, MeOH) *m/z*: 768.4156 [M\* – SbF<sub>6</sub>]<sup>+</sup> (calcd 768.4167); [M\*]<sup>+</sup>: Molecular ion of methanol addition product, [(SIPr)Au(NHC<sub>10</sub>H<sub>15</sub>OMe)]<sup>+</sup>. [(SIPr)Au(4-azahomoadamant-3-ene)][SbF<sub>6</sub>] is a colorless solid, moderately air sensitive. The crystalline solid can be stored for several weeks under an inert atmosphere in a –30 °C refrigerator, but in CD<sub>2</sub>Cl<sub>2</sub> solution showed decomposition after one week when stored in a –10 °C refrigerator. 4-Azahomoadamant-3-ene = 4-azatricyclo[4.3.1.1<sup>3,8</sup>]undec-3-ene.

ant-3-ene)][SbF<sub>6</sub>] is a colorless solid, moderately air sensitive. The crystalline solid can be stored for several weeks under an inert atmosphere in a –30 °C refrigerator, but in CD<sub>2</sub>Cl<sub>2</sub> solution showed decomposition after one week when stored in a –10 °C refrigerator. 4-Azahomoadamant-3-ene = 4-azatricyclo[4.3.1.1<sup>3,8</sup>]undec-3-ene.

[(SIPr)Au(3-methoxy-4-azahomoadamantane)][SbF<sub>6</sub>] ([16][SbF<sub>6</sub>]). A solution of [(SIPr)Au(4-azahomoadamant-3-ene)][SbF<sub>6</sub>] (0.042 g, 0.043 mmol) in mixed solvent dichloromethane/methanol (~12 mL, 5:1) was placed in a 50-mL Schlenk flask. The reaction mixture was heated for 10 h at 50 °C. Solvent was evaporated to dryness under vacuum to yield a white solid. The white solid was redissolved in dichloromethane (3 mL) and layered with hexane (~5 mL) and kept in a refrigerator at –10 °C to obtain a colorless, prism-shaped crystals of [(SIPr)Au(3-methoxy-4-azahomoadamantane)][SbF<sub>6</sub>] (0.026 g, 60% yield). <sup>1</sup>H NMR (CD<sub>2</sub>Cl<sub>2</sub>, 500.16 MHz, 298 K): δ 7.46 (t, 2H, <sup>3</sup>J<sub>HH</sub> = 8 Hz, C<sub>6</sub>H<sub>3</sub>), 7.29 (d, 4H, <sup>3</sup>J<sub>HH</sub> = 8 Hz, C<sub>6</sub>H<sub>3</sub>), 4.19 (s, 4H, CH<sub>2</sub>), 3.04 (m, 4H, CH(CH<sub>3</sub>)<sub>2</sub>), 2.92 (m, 1H, NHC<sub>10</sub>H<sub>15</sub>), 2.69 (s, 3H, OCH<sub>3</sub>), 1.98 (m, 2H, NHC<sub>10</sub>H<sub>15</sub>), 1.79 (m, 6H, NHC<sub>10</sub>H<sub>15</sub>), 1.50 (m, 6H, NHC<sub>10</sub>H<sub>15</sub>), 1.39 (m, 12H, CH(CH<sub>3</sub>)<sub>2</sub>), 1.39 (d, 12H, <sup>3</sup>J<sub>HH</sub> = 8 Hz, CH(CH<sub>3</sub>)<sub>2</sub>). <sup>13</sup>C{<sup>1</sup>H} NMR (CD<sub>2</sub>Cl<sub>2</sub>, 125.77 MHz, 298 K): δ 192.1 (Au–N<sub>3</sub>), 147.3, 147.2, 134.1, 130.6, 125.2, 92.2, 56.5, CH<sub>2</sub> peak overlapped with solvent signal, 49.3, 42.1, 40.8, 37.9, 34.2, 34.1, 32.2, 29.3, 26.5, 25.9, 25.2, 25.1, 24.5, 24.4. IR (crystals, ATR) cm<sup>–1</sup>: 3264 w (NH), 2962 m, 2925 m, 2868 m, 1704 w, 1590 w, 1504 m, 1462 m, 1385 w, 1345 w, 1326 w, 1281 m, 1260 s, 1184 w, 1096 s, 1049 s, 1016 s, 986 w, 864 w, 846 w, 800 m, 706, 655 s, 563 w, 548 w. Anal. Calcd for C<sub>38</sub>H<sub>57</sub>N<sub>3</sub>F<sub>6</sub>AuOSb: C, 45.43; H, 5.72; N, 4.18. Found: C, 45.72; H, 5.98; N, 3.85%. HR-ESI-MS (positive ion, MeOH) *m/z*: 768.4156 [M – SbF<sub>6</sub>]<sup>+</sup> (calcd 768.4167). [(SIPr)Au(3-methoxy-4-azahomoadamantane)][SbF<sub>6</sub>] is a colorless solid, moderately air sensitive. The crystalline solid can be stored for several days under an inert atmosphere at –30 °C refrigerator, but its CD<sub>2</sub>Cl<sub>2</sub> solution showed signs of decomposition if left overnight at room temperature. 3-Methoxy-4-azahomoadamantane = 3-methoxy-4-azatricyclo[4.3.1.1-3,8]undecane.

[(SIPr)Au(4-azahomoadamant-4-ene)][SbF<sub>6</sub>] ([17][SbF<sub>6</sub>]). A solution of [(SIPr)AuN(2-Ad)NN][SbF<sub>6</sub>] (0.53 g, 0.053 mmol) in mixed solvent dichloromethane/hexane (~14 mL, 6:1) was placed in a 50-mL Schlenk flask. The reaction mixture was heated at 50 °C for 6 h. The resulting mixture was concentrated to ~2 mL under reduced pressure. The concentrated solution was layered with hexane (~5 mL) and kept in a refrigerator at –10 °C to obtain colorless, prism-shaped crystals of [(SIPr)Au(4-azahomoadamant-4-ene)][SbF<sub>6</sub>] (0.048 g, 92% yield). Mp: 230–236 °C dec <sup>1</sup>H NMR (CDCl<sub>3</sub>, 500.16 MHz, 298 K): δ 7.67 (d, 1H, <sup>3</sup>J<sub>HH</sub> = 6.9 Hz, NC<sub>10</sub>H<sub>15</sub>), 7.45 (t, 2H, <sup>3</sup>J<sub>HH</sub> = 8 Hz, C<sub>6</sub>H<sub>3</sub>), 7.26 (d, 4H, <sup>3</sup>J<sub>HH</sub> = 8 Hz, C<sub>6</sub>H<sub>3</sub>), 4.25 (s, 4H, CH<sub>2</sub>), 3.45 (m, 1H, NC<sub>10</sub>H<sub>15</sub>), 3.04 (sept, 4H, <sup>3</sup>J<sub>HH</sub> = 6.9 Hz, CH(CH<sub>3</sub>)<sub>2</sub>), 2.82 (m, 1H, NC<sub>10</sub>H<sub>15</sub>), 2.04 (br s, 2H, NC<sub>10</sub>H<sub>15</sub>), 1.62 (m, 8H, NC<sub>10</sub>H<sub>15</sub>), 1.41 (m, 2H, NC<sub>10</sub>H<sub>15</sub>), 1.36 (d, 12H, <sup>3</sup>J<sub>HH</sub> = 6.9 Hz, CH(CH<sub>3</sub>)<sub>2</sub>), 1.33 (d, 12H, <sup>3</sup>J<sub>HH</sub> = 6.9 Hz, CH(CH<sub>3</sub>)<sub>2</sub>). <sup>13</sup>C{<sup>1</sup>H} NMR (CDCl<sub>3</sub>, 125.77 MHz, 298 K): δ 190.6 (Au–N<sub>3</sub>), 186.3 (C=N), 146.9, 133.6, 130.4, 124.8, 63.2, 54.1, 36.5, 34.2, 31.1, 29.0, 28.9, 26.9, 25.3, 24.2; DEPT-135 NMR 186.3 (+ve), 130.4 (+ve), 124.8 (+ve), 63.2 (+ve), 54.1 (–ve), 36.5 (+ve), 34.2 (–ve), 31.1 (–ve), 29.0 (+ve), 28.9 (–ve), 26.9 (+ve), 25.3 (+ve), 24.2 (+ve). IR (crystals, ATR) cm<sup>–1</sup>: 2961 s, 2926 m, 2862 m, 1655 m, 1590 w, 1514 s, 1466 s, 1443 m, 1396 w, 1385 w, 1362 w, 1348 w, 1328 w, 1283 s, 1260 s, 1092 s, 1056 s, 1043 s, 1016 s, 967 w, 953 w, 935 w, 864 w, 801 s, 759 s, 707 w, 654 s, 574 w, 548 w. Anal. Calcd for C<sub>37</sub>H<sub>53</sub>N<sub>3</sub>F<sub>6</sub>AuSb-0.5CH<sub>2</sub>Cl<sub>2</sub>: C, 44.37; H, 5.36; N, 4.14. Found: C, 44.01; H, 5.74; N, 3.79%. HR-ESI-MS (positive ion, MeOH) *m/z*: 736.3884 [M – SbF<sub>6</sub>]<sup>+</sup> (calcd 736.3905). [(SIPr)Au(4-azahomoadamant-4-ene)][SbF<sub>6</sub>] is a colorless air-stable solid. The title compound in CDCl<sub>3</sub> solution showed no signs of decomposition even after 3 days at room temperature. The crystalline solid can be stored for several weeks under an inert atmosphere at room temperature. 4-Azahomoadamant-4-ene = 4-azatricyclo[4.3.1.1<sup>3,8</sup>]undec-4-ene.

[(SIPr)Au(1-azacyclohept-1-ene)][SbF<sub>6</sub>] ([18][SbF<sub>6</sub>]) and [(SIPr)Au(cyclohexanimine)][SbF<sub>6</sub>] ([19][SbF<sub>6</sub>]). A solution of



[(SIPr)AuN(Cy)NN][SbF<sub>6</sub>] (0.054 g, 0.057 mmol) in mixed solvent dichloromethane/hexane (~14 mL, 6:1) was taken in a 50-mL Schlenk flask. The reaction mixture was heated for 6 h at 50 °C. The resulting mixture was concentrated to ~2 mL under reduced pressure. The concentrated solution was layered with hexane (~4 mL) and kept in a refrigerator at -10 °C to obtain colorless, needle-shaped crystals. Solvent was removed using a syringe and the remaining solid was dried under vacuum to obtain white solid (0.045 g, 85% yield); <sup>1</sup>H NMR shows a mixture of complexes [18][SbF<sub>6</sub>] and [19][SbF<sub>6</sub>] in approximately 2:1 ratio). Mp: 195–198 °C dec <sup>1</sup>H NMR (CD<sub>2</sub>Cl<sub>2</sub>, 500.16 MHz, 298 K): (mixture of two isomeric products) δ (major product) 7.57 (t, 1H, <sup>3</sup>J<sub>HH</sub> = 5.7 Hz, CH=N), 7.47 (m, 2H, C<sub>6</sub>H<sub>3</sub>), 7.30 (m, 4H, C<sub>6</sub>H<sub>3</sub>), 4.19 (s, 4H, CH<sub>2</sub>), 3.37 (m, 2H, NC<sub>6</sub>H<sub>11</sub>), 3.04 (m, 4H, CH(CH<sub>3</sub>)<sub>2</sub>), 2.41 (m, 2H, NC<sub>6</sub>H<sub>11</sub>), 1.69 (m, 4H, NC<sub>6</sub>H<sub>11</sub>), 1.36 (m, 24H, CH(CH<sub>3</sub>)<sub>2</sub>), 1.28 (m, 2H, NC<sub>6</sub>H<sub>11</sub>). <sup>13</sup>C{<sup>1</sup>H} NMR (CD<sub>2</sub>Cl<sub>2</sub>, 125.77 MHz, 298 K): (mixture of two isomeric products, selected peak) δ 198.8, 193.7, 191.0, 184.5; DEPT-135 NMR (selected peak) 184.5 (CH=N, +ve). IR (crystals, ATR) cm<sup>-1</sup>: 3296 w (NH), 2953 s, 2922 s, 2854 s, 1656 w, 1589 w, 1504 m, 1461 s, 1377 m, 1365 m, 1344 w, 1323 w, 1278 m, 1265 w, 1228 w, 1184 w, 1101 w, 1055 w, 1034 w, 1017 w, 934 w, 896 w, 859 w, 807 m, 762 w, 736 m, 703 w, 653 s, 575 w, 548 w. Anal. Calcd for C<sub>33</sub>H<sub>49</sub>N<sub>3</sub>F<sub>6</sub>AuSb·0.5CH<sub>2</sub>Cl<sub>2</sub>: C, 41.78; H, 5.23; N, 4.36. Found: C, 41.36; H, 4.98; N, 4.33%. HR-ESI-MS (positive ion, MeOH) *m/z*: 684.3609 [M - SbF<sub>6</sub>]<sup>+</sup> (calcd 684.3592). The mixture of the complexes [18][SbF<sub>6</sub>] and [19][SbF<sub>6</sub>] are colorless solid, moderately air sensitive. The crystalline solid can be stored for several months under an inert atmosphere at -30 °C refrigerator.

**Representative Kinetic Experiment for the Decomposition of [(SIPr)AuN(2-Ad)NN][SbF<sub>6</sub>] ([13][SbF<sub>6</sub>]).** In a Drybox, the complex [13][SbF<sub>6</sub>] (0.003 g, 3 μmol) was dissolved in 0.6 mL of dry CDCl<sub>3</sub> and the resultant solution was transferred to a NMR tube. The NMR tube was inserted into a preheated NMR probe at 50 °C and single-pulse <sup>1</sup>H NMR spectra were recorded at every 30 min. The resonance at 3.89 ppm of [13][SbF<sub>6</sub>] was used to monitor the disappearance of gold(I)-bonded 2-azidoadamantane over time and the formation of the rearrangement product [17][SbF<sub>6</sub>] was indicated by the appearance of a peak at 3.45 ppm. The reactant [13][SbF<sub>6</sub>] and product [17][SbF<sub>6</sub>] amounts were obtained by the integration of the corresponding <sup>1</sup>H NMR signal. The rate constant was calculated from graph ln([13][SbF<sub>6</sub>]) versus time (s) (see Supporting Information).

**X-ray Crystallographic Data.** A suitable crystal covered with a layer of Paratone-N oil, was selected and mounted within a cryo-loop and immediately placed in the low-temperature nitrogen stream. Diffraction data were collected at *T* = 100(2) K. The data sets for [12][SbF<sub>6</sub>], [14][SbF<sub>6</sub>], [15][SbF<sub>6</sub>], [16][SbF<sub>6</sub>] and [18][SbF<sub>6</sub>]/[19][SbF<sub>6</sub>] were collected on a Bruker SMART APEX CCD diffractometer or Bruker SMART APEX II CCD diffractometer with graphite monochromated Mo K $\alpha$  radiation ( $\lambda$  = 0.71073 Å). The data sets for [13][SbF<sub>6</sub>] and [17][SbF<sub>6</sub>] were measured at 100(2) K on a Bruker D8 Quest with a Photon 100 CMOS detector equipped with an Oxford Cryosystems 700 series cooler, a Triumph monochromator, and a Mo K $\alpha$  fine-focus sealed tube ( $\lambda$  = 0.71073 Å). Absorption corrections were applied by using SADABS. Intensity data were processed using the Saint Plus program. Structures were solved with the XS<sup>49</sup> structure solution program using Direct Methods of SHELXTL and refined with the XL<sup>49</sup> refinement package using least-squares minimization within Olex2.<sup>50</sup> Hydrogen atoms were included at calculated positions and refined in a riding manner along with the attached carbons. ORTEP diagrams were generated using Olex2. The CCDC 940336–940339, 942038, and 955397–955398 contain the supplementary crystallographic data. These data can be obtained free of charge via <http://www.ccdc.cam.ac.uk/conts/retrieving.html> or from the Cambridge Crystallographic Data Centre (CCDC), 12 Union Road, Cambridge, CB2 1EZ, UK).

## COMPUTATIONAL METHODS

All computations employed the Gaussian 09 program.<sup>51</sup> Hybrid quantum mechanics/molecular mechanics (QM/MM) calculations, within the ONIOM formalism,<sup>52</sup> were performed on full experimental

chemical models utilizing the BP86<sup>53,54</sup> density functional for the QM region in conjunction with the 6-311+G(d) Pople basis set. Gold was modeled by the Stevens effective core potentials and valence basis sets.<sup>55</sup> The classical MM region was modeled by the Universal Force Field<sup>56</sup> (UFF) and contained the Dipp (Dipp = 2,6-di-isopropyl-phenyl) substituents of SIPr.

Open- and closed-shell species were modeled within the unrestricted and restricted Kohn–Sham theory, respectively. All geometry optimizations were conducted without constraint. The energy Hessian was evaluated at all stationary points to designate them as either minima or transition states at the pertinent levels of theory. Free energies are reported at 298.15 K and 1 atm and are calculated with unscaled vibrational frequencies.

## ASSOCIATED CONTENT

### Supporting Information

Additional figures and X-ray crystallographic data (CIF) for [(SIPr)AuN(1-Ad)NN][SbF<sub>6</sub>] ([12][SbF<sub>6</sub>]), [(SIPr)AuN(2-Ad)NN][SbF<sub>6</sub>] ([13][SbF<sub>6</sub>]), [(SIPr)AuN(Cy)NN][SbF<sub>6</sub>] ([14][SbF<sub>6</sub>]), [(SIPr)Au(4-azahomoadamant-3-ene)][SbF<sub>6</sub>] ([15][SbF<sub>6</sub>]), [(SIPr)Au(3-methoxy-4-azahomoadamantane)][SbF<sub>6</sub>] ([16][SbF<sub>6</sub>]), [(SIPr)Au(4-azahomoadamant-4-ene)][SbF<sub>6</sub>] ([17][SbF<sub>6</sub>]), [(SIPr)Au(1-azacyclohept-1-ene)][SbF<sub>6</sub>] ([18][SbF<sub>6</sub>])/[(SIPr)Au(cyclohexanimine)][SbF<sub>6</sub>] ([19][SbF<sub>6</sub>]). <sup>1</sup>H/<sup>13</sup>C HMBC spectrum of compounds [15][SbF<sub>6</sub>], [17][SbF<sub>6</sub>], [18][SbF<sub>6</sub>]/[19][SbF<sub>6</sub>] and computational results. This material is available free of charge via the Internet at <http://pubs.acs.org>.

## AUTHOR INFORMATION

### Corresponding Author

dias@uta.edu; t@unt.edu

### Notes

The authors declare no competing financial interest.

## ACKNOWLEDGMENTS

This work was supported by the National Science Foundation (CHE-0845321 and CHE-1265807) and the Robert A. Welch Foundation (Grant Y-1289). We thank Charles Savage for his help in collecting low- and high-temperature NMR spectroscopic data and Maciej Kukula for collecting MS spectroscopic data. T.R.C. acknowledges partial support of this research by the U.S. Department of Energy (DE-FG02-03ER15387).

## REFERENCES

- (1) L'Abbé, G. *Chem. Rev.* **1969**, *69*, 345–363.
- (2) Kyba, E. P. *Alkyl Azides and Nitrenes*; Academic Press: Orlando, FL, 1984; pp 1–34.
- (3) Scriven, E. F. V.; Turnbull, K. *Chem. Rev.* **1988**, *88*, 297–368.
- (4) Brase, S.; Gil, C.; Knepper, K.; Zimmermann, V. *Angew. Chem., Int. Ed.* **2005**, *44*, 5188–5240.
- (5) *Organic Azides: Syntheses and Applications*; Brase, S., Banert, K., Eds.; John Wiley & Sons Ltd.: Chichester, 2010.
- (6) *Photochemistry of Azides: the Azide/Nitrene Interface*; Gritsan, N., Platz, M., Eds.; John Wiley & Sons Ltd.: Chichester, 2010.
- (7) Gephart, R. T.; Warren, T. H. *Organometallics* **2012**, *31*, 7728–7752.
- (8) Wiese, S.; McAfee, J. L.; Pahls, D. R.; McMullin, C. L.; Cundari, T. R.; Warren, T. H. *J. Am. Chem. Soc.* **2012**, *134*, 10114–10121.
- (9) Harman, W. H.; Lichterman, M. F.; Piro, N. A.; Chang, C. J. *Inorg. Chem.* **2012**, *51*, 10037–10042.
- (10) Driver, T. G. *Org. Biomol. Chem.* **2010**, *8*, 3831–3846.
- (11) Dunkin, I. R.; Shields, C. J.; Quast, H.; Seiferling, B. *Tetrahedron Lett.* **1983**, *24*, 3887–3890.

- (12) Radziszewski, J. G.; Downing, J. W.; Jawdosiuik, M.; Kovacic, P.; Michl, J. *J. Am. Chem. Soc.* **1985**, *107*, 594–603.
- (13) Bock, H.; Dammel, R. *J. Am. Chem. Soc.* **1988**, *110*, 5261–5269.
- (14) Brinker, U. H.; Walla, P.; Krois, D.; Arion, V. B. *Eur. J. Org. Chem.* **2011**, 1249–1255.
- (15) Choudhury, R.; Gupta, S.; Da, S. J. P.; Ramamurthy, V. *J. Org. Chem.* **2013**, *78*, 1824–1832.
- (16) Margosian, D.; Kovacic, P. *J. Org. Chem.* **1981**, *46*, 877–880.
- (17) An, D.; Wang, J.; Dong, T.; Yang, Y.; Wen, T.; Zhu, H.; Lu, X.; Wang, Y. *Eur. J. Inorg. Chem.* **2010**, 4506–4512.
- (18) Dias, H. V. R.; Polach, S. A.; Goh, S.-K.; Archibong, E. F.; Marynick, D. S. *Inorg. Chem.* **2000**, *39*, 3894–3901.
- (19) Barz, M.; Herdtweck, E.; Thiel, W. R. *Angew. Chem., Int. Ed.* **1998**, *37*, 2262–2265.
- (20) Proulx, G.; Bergman, R. G. *J. Am. Chem. Soc.* **1995**, *117*, 6382–6383.
- (21) Fickes, M. G.; Davis, W. M.; Cummins, C. C. *J. Am. Chem. Soc.* **1995**, *117*, 6384–6385.
- (22) Proulx, G.; Bergman, R. G. *Organometallics* **1996**, *15*, 684–692.
- (23) Hanna, T. A.; Baranger, A. M.; Bergman, R. G. *Angew. Chem., Int. Ed. Engl.* **1996**, *35*, 653–655.
- (24) Brotherton, W. S.; Guha, P. M.; Phan, H.; Clark, R. J.; Shatruck, M.; Zhu, L. *Dalton Trans.* **2011**, *40*, 3655–3665.
- (25) Mankad, N. P.; Mueller, P.; Peters, J. C. *J. Am. Chem. Soc.* **2010**, *132*, 4083–4085.
- (26) Waterman, R.; Hillhouse, G. L. *J. Am. Chem. Soc.* **2008**, *130*, 12628–12629.
- (27) Albertin, G.; Antoniutti, S.; Baldan, D.; Castro, J.; Garcia-Fontan, S. *Inorg. Chem.* **2008**, *47*, 742–748.
- (28) Guillemot, G.; Solari, E.; Floriani, C.; Rizzoli, C. *Organometallics* **2001**, *20*, 607–615.
- (29) Cenini, S.; Gallo, E.; Caselli, A.; Ragaini, F.; Fantauzzi, S.; Piangiolino, C. *Coord. Chem. Rev.* **2006**, *250*, 1234–1253.
- (30) Partyka, D. V.; Robilotto, T. J.; Updegraff, J. B., III; Zeller, M.; Hunter, A. D.; Gray, T. G. *Organometallics* **2009**, *28*, 795–801.
- (31) Harrold, N. D.; Waterman, R.; Hillhouse, G. L.; Cundari, T. R. *J. Am. Chem. Soc.* **2009**, *131*, 12872–12873.
- (32) Cundari, T. R.; Pierpont, A. W.; Vaddadi, S. *J. Organomet. Chem.* **2007**, *692*, 4551–4559.
- (33) Eckert, N. A.; Vaddadi, S.; Stoian, S.; Lachicotte, R. J.; Cundari, T. R.; Holland, P. L. *Angew. Chem., Int. Ed.* **2006**, *45*, 6868–6871.
- (34) Kogut, E.; Wiencko, H. L.; Zhang, L.; Cordeau, D. E.; Warren, T. H. *J. Am. Chem. Soc.* **2005**, *127*, 11248–11249.
- (35) Wiese, S.; Aguila, M. J. B.; Kogut, E.; Warren, T. H. *Organometallics* **2013**, *32*, 2300–2308.
- (36) Cowley, R. E.; Eckert, N. A.; Elhaik, J.; Holland, P. L. *Chem. Commun.* **2009**, 1760–1762.
- (37) Aguila, M. J. B.; Badiei, Y. M.; Warren, T. H. *J. Am. Chem. Soc.* **2013**, *135*, 9399–9406.
- (38) Badiei, Y. M.; Dinescu, A.; Dai, X.; Palomino, R. M.; Heinemann, F. W.; Cundari, T. R.; Warren, T. H. *Angew. Chem., Int. Ed.* **2008**, *47*, 9961–9964.
- (39) Laskowski, C. A.; Morello, G. R.; Saouma, C. T.; Cundari, T. R.; Hillhouse, G. L. *Chem. Sci.* **2013**, *4*, 170–174.
- (40) Li, Z.; Brouwer, C.; He, C. *Chem. Rev.* **2008**, *108*, 3239–3265.
- (41) Li, Z.; Capretto, D. A.; Rahaman, R. O.; He, C. *J. Am. Chem. Soc.* **2007**, *129*, 12058–12059.
- (42) Li, Z.; Ding, X.; He, C. *J. Org. Chem.* **2006**, *71*, 5876–5880.
- (43) Besora, M.; Harvey, J. N. *J. Chem. Phys.* **2008**, *129*, 044303/1–044303/10.
- (44) Kreher, R.; Jäger, G. *Z. Naturforsch., B: Chem. Sci.* **1964**, *19*, 657–658.
- (45) Stüss-Fink, G.; Khan, L.; Raithby, P. R. *J. Organomet. Chem.* **1982**, *228*, 179–189.
- (46) De Frémont, P.; Scott, N. M.; Stevens, E. D.; Nolan, S. P. *Organometallics* **2005**, *24*, 2411–2418.
- (47) Prakash, G. K. S.; Stephenson, M. A.; Shih, J. G.; Olah, G. A. *J. Org. Chem.* **1986**, *51*, 3215–3217.
- (48) Maury, J.; Feray, L.; Bertrand, M. P.; Kapat, A.; Renaud, P. *Tetrahedron* **2012**, *68*, 9606–9611.
- (49) Sheldrick, G. M. *Acta Crystallogr.* **2008**, *A64*, 112–122.
- (50) Dolomanov, O. V.; Bourhis, L. J.; Gildea, R. J.; Howard, J. A. K.; Puschmann, H. *J. Appl. Crystallogr.* **2009**, *42*, 339–341.
- (51) Frisch, M. J. *Gaussian 09*, Revision B.01; Gaussian, Inc.: Wallingford CT, 2009.
- (52) Svensson, M.; Humbel, S.; Froese, R. D. J.; Matsubara, T.; Sieber, S.; Morokuma, K. *J. Phys. Chem.* **1996**, *100*, 19357–19363.
- (53) Becke, A. D. *Phys. Rev. A* **1988**, *38*, 3098–3100.
- (54) Perdew, J. P. *Phys. Rev. B* **1986**, *33*, 8822–8824.
- (55) Stevens, W. J.; Krauss, M.; Basch, H.; Jasien, P. G. *Can. J. Chem.* **1992**, *70*, 612–630.
- (56) Rappe, A. K.; Casewit, C. J.; Colwell, K. S.; Goddard, W. A., III; Skiff, W. M. *J. Am. Chem. Soc.* **1992**, *114*, 10024–10025.